Journal of Thermal Analysis and Calorimetry (2023) 148:293–304
https://doi.org/10.1007/s10973-022-11712-x

Effect of clay minerals on the flame retardancy of polylactic acid/ammonium polyphosphate system

Thuy Tien Nguyen Thanh[1] · Beáta Szolnoki[1] · Dániel Vadas[1] · Milán Nacsa[1] · György Marosi[1] · Katalin Bocz[1]

Received: 31 May 2022 / Accepted: 11 October 2022 / Published online: 4 November 2022

Abstract

The overview of the literature reveals the lack of comprehensive study on the effect of clay minerals in flame-retarded polylactic acid (PLA) composites. This research focuses on sepiolite (SEP) and montmorillonite (MMT) clay minerals and their impact on ammonium polyphosphate (APP)-based intumescent flame-retardant (IFR) system in PLA. The effects of the clay mineral types, their surface modification (O-SEP and O-MMT, respectively) and their concentration in PLA/APP composites on the flame-retardant properties were comprehensively evaluated through thermal and flammability tests. Overall, the sepiolite-containing samples showed the greatest decrease in pHRR and THR values at the 3 m/m% loading level. The sepiolites showed stronger interfacial interactions with the PLA matrix than the montmorillonites, and the organomodification proved to improve the compatibility of both types of clay minerals according to the dynamic mechanical analysis (DMA) results. Yet, the organomodification had a contradictory effect on the flame-retardant properties. In the case of sepiolites, it proved to be beneficial as the O-SEP added composite achieved a 60% decrease in the pHRR value and reduced the THR value to 60%. For montmorillonites, the improved compatibility by the organomodification with the PLA matrix seemed to hinder its flame-retardant effectiveness, as the critical point to its flame-retardant mechanism is the rapid migration and accumulation of the clay minerals towards the surface of the polymer.

Keywords Clay minerals · Sepiolite · Montmorillonite · Polylactic acid · Intumescent flame retardant

Introduction

Polymers derived from renewable resources are increasingly used in the plastic industry due to their environmental benefits. Among the biobased polymers, polylactic acid (PLA) has received increasing attention in recent years [1–4]. It has been applied in the packaging and fibre industry, where the fire safety is not a priority, so initially, there was no need for enhancing the flame retardancy of PLA. As soon as it became a promising alternative to even durable petrochemical thermoplastics due to its good mechanical properties alongside its renewability, biodegradability and biocompatibility [5], considerable efforts have been made to improve the fire resistance of PLA. Even though these PLA-based engineering products require a remarkable flame-retardant grade to meet safety standards, they are increasingly applied in the automotive, electrical and aerospace industries and building materials [6–9].

The high flammability of PLA is due to its molecular structure: It can be easily ignited, and the severe dripping does not only increase the surface accessible for the flame, but it can also easily ignite flammable materials nearby, and the further spread of flames results in fire accidents [3, 10, 11]. Due to its high burning rate, neat PLA cannot be categorized by UL94, and it has a low 19–21 v/v% LOI value [12–14]. In the case of PLA, intumescent flame retardants (IFRs) are a promising way to reduce its flammability [12]. The advantages of IFR are suppressed heat emission, reduced smoke production, decreased release of toxic gases and less dripping of molten PLA as a result of the charred protective layer formed on the surface of the polymer [14]. The flame retardancy of IFR systems can be enhanced by the application of micro- and nanoscale particles that can significantly improve the properties of materials at relatively low concentrations due to the large surface area,

✉ Beáta Szolnoki
szolnoki.beata@vbk.bme.hu

[1] Department of Organic Chemistry and Technology, Faculty of Chemical Technology and Biotechnology, Budapest University of Technology and Economics, Műegyetem Rkp. 3, 1111 Budapest, Hungary

which increases the surface contact area with the polymer matrix [15]. The greatest improvements were achieved when the nanoparticles were finely and uniformly dispersed and showed strong affinity towards the corresponding polymer matrix [14]. Several studies showed that the layered silicates at low loading (1–5 m/m%) could increase the thermal stability while decreasing the flammability of the polymer at the same time [16–18].

In the case of PLA, besides the improved affinity and reinforcing effect, these additives also act as a potential synergist for flame retardants by enhancing the formation of a thermal insulation layer on the surface of the burning matter. Such materials are expandable graphite, halloysite, carbon nanotubes and mineral clays. Montmorillonite (MMT) and sepiolite (SEP) are mineral clays, montmorillonite has a platelet-like form, and sepiolite clays are needle-like fibrous fillers. Fibrous fillers with lower specific surface area are believed to be more easily dispersible than platelet-like fillers [19]. On the other hand, due to their morphology, the plate-like clays could create a more continuous surface layer, which could be advantageous in improving the oxygen barrier properties of the polymer [20]. *Pluta* et al. concluded that the nature of the filler affects the ordering of the PLA matrix at the molecular and supermolecular levels. The mineral clays readily interact with the polymer matrix during blending, leading to the formation of at least an intercalated structure [21]. Using a minimal additional amount, they could significantly improve the barrier performance, promote char formation, enhance the polymer composite's thermal stability and thus reduce flammability [13],13].

Li et al. reported on the effect of organomodified montmorillonite (O-MMT) in APP flame-retarded PLA at 5 m/m% loading [23]. The morphological analysis of the char layer showed an integrated honeycomb pore structure. During combustion, the clay significantly enhanced the melt stability of the composite and effectively suppressed the melt dripping. *Isitman* et al. proposed a possible mechanism for O-MMT in forming the charred layer [24]. They assumed that the O-MMT platelets become incompatible with the polymer matrix during combustion. This results in rapid migration and accumulation of the clay on the surface and forming the charred layer on the polymer. *Bourbigot* and *Fontaine* [25] also examined the addition of O-MMT at 1 m/m% loading to APP flame-retardant and melamine-containing PLA, where the synergic effect of the clay was observed. They concluded that the clay reacts with the APP through the formation of aluminophosphate species which then thermally stabilize the structure, thus resulting in a more cohesive char. *He* et al. [26] proposed that in the composites, the PLA molecules are more orderly arranged, and this rigidity effectively inhibits the movements of molecular chains. This hinders the migration of small molecules generated by pyrolysis and thus improves the thermal stability of the composite. *Ramesh* et al. [27] investigated the effect of MMT clay on aloe vera fibre-treated PLA biocomposite, where the optimum content of MMT was found to be 1 m/m% for appropriate fire retardancy, whereas higher loading showed voids and agglomeration in the polymer matrix and decreased mechanical strength.

SEP was investigated in multiwalled nanotubes (MWNT)-reinforced PLA [28], where it was observed that the needle-like shape helps the flowability of the polymer during melt processing. The stacked needle structure of SEP in the polymer could also hold accumulated heat which could be used as a heat source to accelerate the decomposition process simultaneously with the heat flow supplied by the heat source outside [29]. The MWNT-reinforced PLA composite showed some porosity, but the addition of SEP created a tighter network during heating. The formed char could better hinder the diffusion of volatile decomposition products, thus improving the flame-retarding mechanism. *Liu* et al. [30] prepared PLA clay composites with unmodified (SEP) and organomodified ones (O-SEP) through the solution casting method. They concluded that even though both SEP nanofibres are well dispersed in the PLA matrix, only the unmodified SEP showed improved thermal properties, while O-SEP had even worse flammability results than the pure PLA. They proposed that the traditional organic modification of sepiolite is unnecessary.

On the other hand, *Tang* et al. [5] investigated the efficiency of O-SEP on the PLA intumescent flame-retarded with APP and MA in a 2:1 ratio. The O-SEP/APP-MA additive system enhanced the carbonization of PLA to form the charred layer with high yield and good thermal properties, and the 2 m/m% loading of O-SEP gave the best results, while higher loading displayed relatively poor distribution and poor flame-retardant behaviours. The sample with lower O-SEP content showed a continual, smooth and compact outer char surface, while the inner surface exhibited a honeycomb-like structure. This could suppress the mass and heat transfer and effectively retard the burning of underlying materials. However, the higher loading showed less solid and more pores on the surface, resulting in insufficient char formation and a less compact char layer during the burning. *Jiang* et al. [19] also concluded that sepiolite clays are easily dispersible due to their lower specific surface area, and O-SEP is more effective in creating optimal interphase between the matrix and clays due to the organic modification, and this can further improve the composite properties.

Several papers concluded that the higher loading of the clays has a negative impact on the composites' properties [31–34]. *Guo* et al. [32] experienced that the enhanced performance occurs only within a very narrow composition window in MMT-loaded PLA. The loading of 1 m/m% drastically altered the morphology, and the matrix's domain size increased but still maintained its

structure and distribution. At higher loading of 2 m/m%, the investigated domains became elongated, and the excess clay aggregated within the domains, decreasing its effectiveness. *Hazer* et al. [33] observed that the increasing clay loading level causes voids in the matrix and aggregation of clays, and they assumed that this results in brittle formation due to the stiff nature, thus decreasing the flame-retardant and mechanical properties of the composite. *Norouzi* et al. [34] proposed another explanation for the poor qualities of higher clay content. They assumed that the re-assembling of the nanoparticle layers might hinder the ammonia gas from swelling the char, which has a negative impact on the fire retardation.

Some research also focussed on comparing MMT and SEP clays with each other. *González* et al. [35] focussed on the synergic effect of both O-MMT and neat sepiolite, and they concluded that the enhanced interrelationship resulted from the H-bonding of carbonyl groups to the treating agent's hydroxyl groups within the matrix. This compatibility causes the great dispersion of clays in the matrix. *Fukushima* et al. [20] also found a good dispersion of O-MMT and SEP clays in the PLA polymer matrix and observed the formation of an interconnected structure within the PLA matrix. They inspected that only O-MMT could decrease the oxygen permeability of PLA due to its platelet-like structure, which could make a continuous layer, while the SEP lacks the barrier effect due to its needle-like morphology. *Isitman* et al.'s observation of nanoparticle geometry [36] also concluded that the flame-retarding performance increased from needle-like to platelet-like structures, attributed to nanoparticles' effective surface area in the composites.

The overview of the literature reveals the lack of comprehensive understanding of montmorillonite and sepiolite clay minerals containing flame-retarded PLA composites. No clear conclusion can be derived about whether the organomodification of the clay minerals is beneficial or disadvantageous regarding the interactions and their effect on fire retardancy. The concentration dependency of the properties and the role of the test methods examining different aspects of the materials also need clarification. There is also a lack of detailed comparison of montmorillonite and sepiolite clay minerals at the same concentration and composite system. This study aimed to thoroughly investigate the synergic effect of the co-added clays on the flame retardancy of the biopolymer. We focussed on the addition of nonmodified and organomodified sepiolite or montmorillonite to PLA composites—containing APP as the IFR component—and investigated how the loading amount and the type and the modification of clays affect the flame retardant and properties of the PLA/APP system.

Methodology

Materials

Ingeo™ Biopolymer 2003D-type extrusion grade PLA, supplied by NatureWorks LLC (Minnetonka, MN, USA), was applied as the polymer matrix material. Exolit® AP462-type ammonium polyphosphate microencapsulated with melamine resin, received from Clariant GmbH (Frankfurt am Main, Germany), was applied as an intumescent flame retardant.

PANGEL S9 sepiolite and PANGEL B20 organomodified sepiolite, supplied by TOLSA GROUP (Madrid, Spain), and Nanofil (Cloisite) 116 montmorillonite and Cloisite 20A organomodified montmorillonite, supplied by BYK Additives & Instruments (member of ALTANA, Wesel, Germany), were used as clay mineral co-additive components.

Preparation of composites

Kneading

PLA granules, APP flame-retardant and clay minerals were dried at 70 °C overnight before kneading. The flame-retarded PLA composites were prepared in a Brabender Plastograph-type internal mixer (Brabender GmbH & Co. KG, Duisburg, Germany). The temperature was set to 180 °C and the PLA granules were fed, mixed with the AP462 flame-retardant additive and the clay with the rotor speed of 10 min^{-1}. When the mixture had reached the molten state, the rotor speed was increased to 50 min^{-1} for 10 min.

Moulding

The kneaded mixture was then hot-pressed using a Collin Teach-Line Platen Press 200E-type heated press (Dr. Collin GmbH, München, Germany). About 50 g of each mixed sample was heated to 180 °C in a mould of $100 \times 100 \times 4$ mm^3 size, pressed under 50 bar for 5 min and then let to cool down to room temperature under 50 bar. The specimens for flammability and mechanical testing were obtained by cutting the moulded samples with a bandsaw.

Characterization methods

Thermogravimetric analysis (TGA)

TGA measurements were taken using a TA Instruments Q5000 Apparatus (TA Instruments LLC, New Castle, NH, USA) under 25 mL min^{-1} nitrogen gas flow. Samples of about 10 mg were positioned in open alumina pans. The

samples were heated from 25 to 600 °C by a heating ramp of 10 °C min^{-1} (the precision of the temperature measurements is ± 1.5 °C in the temperature range of 25–800 °C).

UL94

Standard UL94 flammability tests were performed according to ISO 9772 and ISO 9773; the specimen dimensions for the test were 100 × 10 × 4 mm^3.

Limiting oxygen index (LOI)

LOI was determined on specimens with 100 × 10 × 4 mm^3 dimensions according to ISO 4589 standard using an apparatus made by Fire Testing Technology Ltd. (East Grinstead, West Sussex, UK).

Mass loss calorimetry (MLC)

MLC tests were carried out by an instrument delivered by Fire Testing Technology Ltd. (East Grinstead, West Sussex, UK), using the ISO 13927 standard method. Specimens (with 100 × 100 × 4 mm^3 dimensions) were exposed to a constant heat flux of 50 kW m^{-2}, simulating a harsh fire scenario. The ignition was provided by a spark plug located 13 mm above the sample. The main characteristic of fire properties, including heat release rate (HRR) as a function of time, time to ignition (TTI) and total heat release (THR) was determined.

Scanning electron microscopy (SEM)

The charred layer of composites for SEM images was prepared in MLC. Specimens with 30 × 30 × 4 mm^3 dimensions were exposed to the constant heat flux of 50 kW m^{-2} with initial ignition for 3 min until the charred layer was formed. SEM images of the charred layer were taken using a JEOL JSM-5500 LV-type apparatus (JEOL Ltd., Akishima, Tokyo, Japan) at an accelerating voltage of 10 keV. Before the examination, all the samples were sputter-coated with a conductive gold layer to prevent charge build-up on the surface.

Dynamic mechanical analysis

DMA was performed using a Q800 dynamic mechanical analyser (DMA, TA Instruments Inc., New Castle, DE, USA) to determine the storage modulus and loss modulus as a function of temperature for the prepared PLA samples. Dual cantilever mode was applied with a span length of 35 mm. The width and length of the specimens were approximately 10 mm and 60 mm, respectively. The scanning range of temperature was 25–150 °C; a heating rate of 2 °C min^{-1} and a frequency of 1 Hz with a 0.02% deformation were selected.

Results and discussion

The aim of this study was to investigate the flammability differences of PLA/APP intumescent flame-retarded systems combined with organomodified (O-SEP and O-MMT) and nonmodified (SEP and MMT) clay minerals. The loading of APP was kept constant at 15.0 m/m% in the composites, while the clay minerals were added at varying loading levels of 0.5, 1.5 and 3.0 m/m%. The formulations of PLA/APP composites are shown in Table 1. PLA combined with APP at the loading of 15.0 m/m% was used as the reference sample [37].

Dynamic mechanical analysis

DMA, an important characterization tool for the viscoelastic behaviour of polymers and composites [38], provides information about the interfaces of multicomponent systems. The tan δ, a ratio of loss to storage modulus, indicates the energy dissipation potential in relation to molecular mobility and friction at the interfacial region. Increased interfacial interaction imposes restrictions against the local molecular motion (due to the adsorption of polymer chain on the surface of the particles) and frictional energy dissipation, decreasing this way the area under the tan δ curve. The interfacial interactions between the additives and the matrix are significant in determining the bulk properties [39]. The plotted tan δ curves of the samples are shown in Fig. 1. The glass transition temperature (T_g) of the PLA/APP reference sample was found to be 67.5 °C. The addition of the clays

Table 1 Composition of the reference sample and the composites

Sample name	PLA/m/m%	APP/m/m%	Clay/m/m%
PLA/APP reference	85.0	15.0	0.0
0.5% MMT + PLA/APP	84.5	15.0	0.5
1.5% MMT + PLA/APP	83.5	15.0	1.5
3.0% MMT + PLA/APP	82.0	15.0	3.0
0.5% O-MMT + PLA/APP	84.5	15.0	0.5
1.5% O-MMT + PLA/APP	83.5	15.0	1.5
3.0% O-MMT + PLA/APP	82.0	15.0	3.0
0.5% SEP + PLA/APP	84.5	15.0	0.5
1.5% SEP + PLA/APP	83.5	15.0	1.5
3.0% SEP + PLA/APP	82.0	15.0	3.0
0.5% O-SEP + PLA/APP	84.5	15.0	0.5
1.5% O-SEP + PLA/APP	83.5	15.0	1.5
3.0% O-SEP + PLA/APP	82.0	15.0	3.0

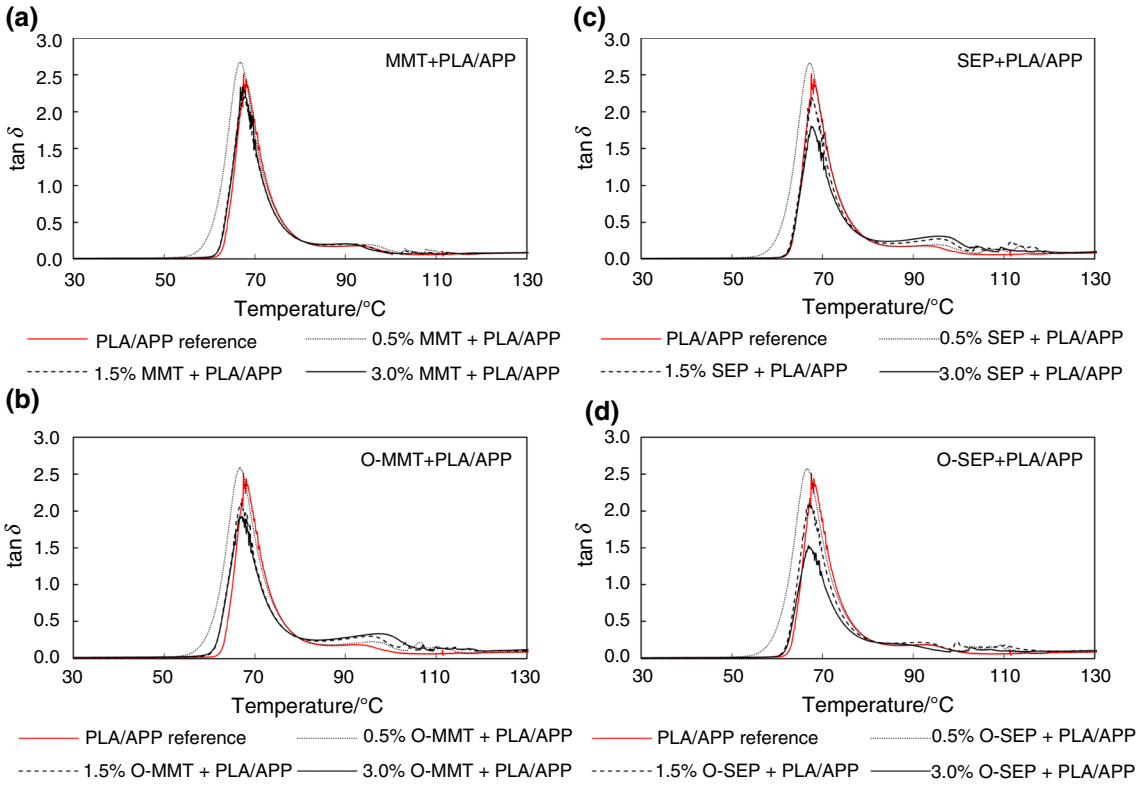

Fig. 1 DMA of the PLA/APP reference samples and the clay-incorporated composites; **a** MMT + PLA/APP, **b** O- MMT + PLA/APP; **c** SEP + PLA/APP; **d** O-SEP + PLA/APP

had an insignificant impact on the value of T_g; however, the increasing loading level decreased the tan δ peaks to varying degrees.

In most cases, the tan δ peak became smaller at higher filler content, indicating increased interfacial adhesion between the flame-retarded matrix and the clay minerals. The MMT clay-containing samples are the exceptions, as their peaks did not show any significant change compared to the reference sample. The greater effect in the tan δ peak for O-MMT and O-SEP samples indicates that the surface modification can significantly improve the compatibility between the clay minerals and the PLA matrix.

When comparing the fibrous and platelet form of the clays, it can be clearly seen that the SEP and O-SEP samples had the lowest tan δ peaks comparably, signifying that the fibrous form is beneficial to achieve strong interactions with the polymer. The observed better compatibility with the PLA matrix for the sepiolite-type clays, especially for O-SEP, may result in better synergistic flame-retardant properties for the composites.

Mass loss calorimetry

As seen in Fig. 2, all flame-retarded PLA samples showed intumescent char formation within the first minutes after ignition. From the heat release rate curve recorded on PLA/APP reference sample, it is interpreted that the charred layer was formed in a relatively short time, which reduced the intensity of the heat released, and the sample reached the pHRR value of 339 kWm^{-2}. In comparison, the composites containing clay minerals showed an enormous suppression in the heat release as soon as the char was formed, reducing the flammability of the samples more effectively than the clay-free reference sample. As the filler content increased in the PLA matrix, the curves became flatter and elongated as the burning became less intense and prolonged in time. Overall, the incorporation of clay fillers showed improved flame retardancy with the APP intumescent flame retardant in PLA composite.

The fibrous structure of the clay is beneficial as the flattest heat release curves belong to the SEP and O-SEP containing composites. According to the MLC results of the composites (Table 2), the maximum heat emission values decreased by 40–60% compared to the reference sample, while the total amount of heat emitted during combustion was reduced to 50–60% at most. The O-SEP clay-incorporated samples showed the most improvements among the composites, having the lowest maximum peak heat released value and the lowest total heat released value at the loading level of 3.0 m/m%. This corresponds to the results of DMA, where

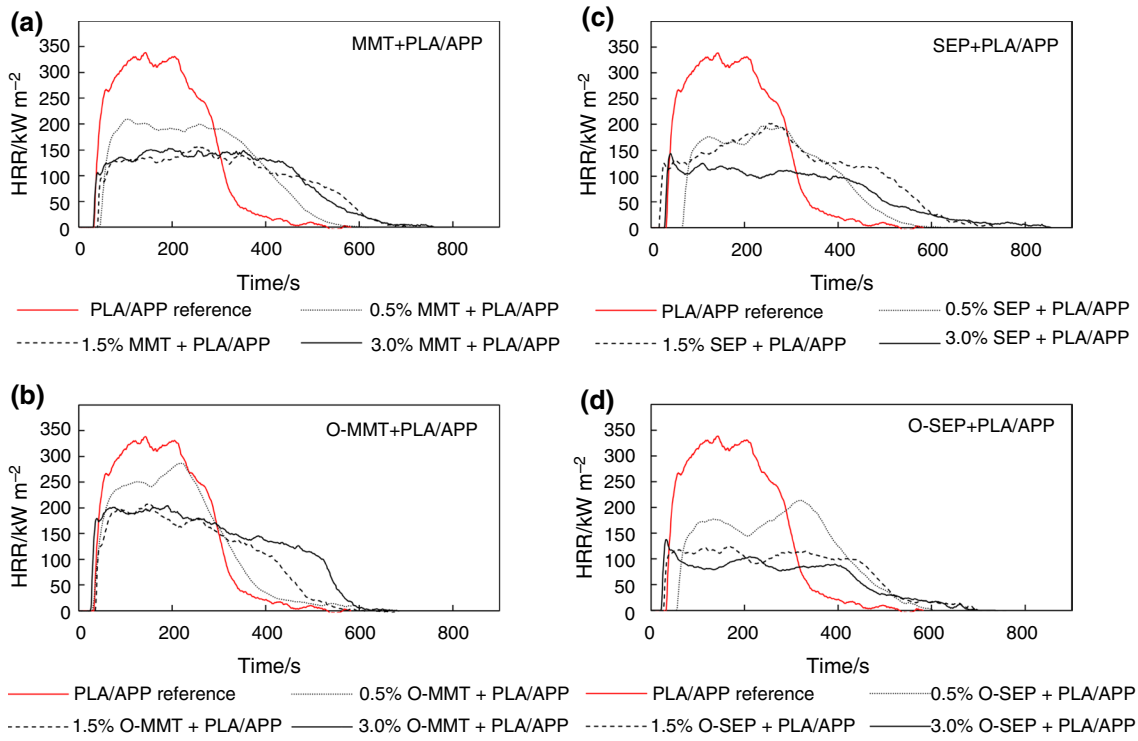

Fig. 2 MLC curves of the PLA/APP reference sample and clay-incorporated composites; **a** MMT + PLA/APP, **b** O-MMT + PLA/APP; **c** SEP + PLA/APP; **d** O-SEP + PLA/APP

Table 2 The results of MLC for the PLA/APP reference sample and the clay-incorporated PLA/APP composites

Sample	TTI/s	pHRR/kWm^{-2}	THR MJ m^{-2}	Residue/%
PLA/APP reference	33	339	81	3
0.5% MMT + PLA/APP	44	209	71	13
1.5% MMT + PLA/APP	41	156	65	14
3.0% MMT + PLA/APP	32	153	68	17
0.5% O-MMT + PLA/APP	43	286	74	11
1.5% O-MMT + PLA/APP	36	209	67	11
3.0% O-MMT + PLA/APP	25	205	84	12
0.5% SEP + PLA/APP	51	200	63	11
1.5% SEP + PLA/APP	18	202	78	14
3.0% SEP + PLA/APP	29	144	54	15
0.5% O-SEP + PLA/APP	43	198	68	12
1.5% O-SEP + PLA/APP	27	125	52	21
3.0% O-SEP + PLA/APP	22	138	43	26

the O-SEP samples showed the greatest compatibility within the PLA matrix, suggesting that well-dispersed fibrous clay improves the quality of the charred barrier structure.

Interestingly, the O-MMT-containing composites had the highest pHRR and THR value among the clay-containing samples at a given loading level and had the lowest residual mass, thus showing the poorest flame-retardant behaviour in the PLA/APP clay composite. Even though O-MMT samples showed better adhesion to the polymer chains in the DMA, in the flammability tests, this better compatibility resulted in worse performance than that of the nonmodified one, as the MMT-containing samples achieved lower pHRR and THR values, while it yielded higher residual mass. This could be explained by the mechanism proposed in the literature for montmorillonite-type clay minerals, assuming rapid migration and accumulation of the clay on the surface during combustion due to clays collapse and the growing incompatibility with the polymer matrix [24]. When the accumulated

clay on the surface is exposed to excessive heat flow, the rapid formation of a charred barrier begins with the APP particles. Due to the weaker adhesion in the PLA matrix, the MMT clays can migrate better and accumulate more towards the surface, significantly suppressing the heat emission. As O-MMT has better compatibility with the PLA matrix, this hinders its migration to the surface, resulting in worse flame-retardant properties.

In the case of sepiolites, the literature proposed that the well-dispersed fine filaments attribute to the efficient flame-retardant properties through promoting homogeneous carbonization of the molten polymer matrix and accelerating the charring process simultaneously from inside with the heat flow supplied by the heat source outside [29]. The organomodification of sepiolite seemed to be beneficial as the O-SEP clay could be dispersed more evenly in the PLA matrix, resulting in the strongest interfacial interaction observed in the DMA. The enhanced charring effect yields the highest residual masses after combustion, along with the lowest pHRR and THR values among the clay mineral-containing composites.

During combustion, the formation of several large cells within the charred layer attributes to the effective barrier effect of intumescent flame retardants [22, 23]. In Fig. 3, the microscopic images of the cross section of the charred composites are shown for the 1.5 m/m% MMT + PLA/APP and 3.0 m/m% O-SEP + PLA/APP samples. Uniform large cells can be observed with additional smaller cell structures in the depth. For the montmorillonites-incorporated samples, the small cells have a honeycomb-like coherent porous structure, while the sepiolite-containing nanocomposites show a more concise and cohesive cellular structure with a thin web-like mesh layer.

The improved flame-retardant performance of the composites with clay minerals could be ascribed to the presence of these small porous cell structures that enhance the barrier effect of the charred layer. Moreover, in the case of sepiolites, it is assumed that the web-like mesh layer helps hold the structure together, strengthening the whole material during combustion and resulting in better flame retardancy.

In contrast to the previous results for maximum and total heat release values and residual mass, as the clay mineral content decreased from 3.0 to 0.5 m/m%, the samples required a longer time to ignite. It shows that the lower loading of the clay minerals-containing composites were most difficult to ignite, while the higher clay mineral content reduced the TTI of the PLA composites, and a similar trend was observed in the LOI test (see chapter 3.4.).

Thermogravimetric analysis

Figure 4 shows the TGA curves obtained in N_2 atmosphere, which enables the investigation of the degradation process

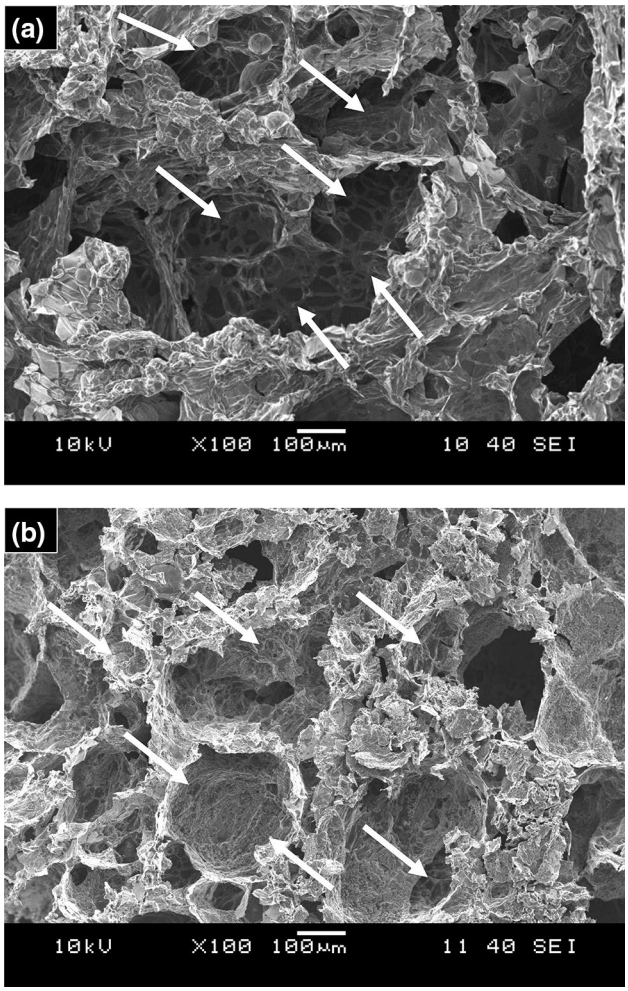

Fig. 3 SEM images of the formed charred protective layer at 100× magnification: **a** 1.5 m/m% MMT + PLA/APP composite; **b** 3.0 m/m% O-SEP + PLA/APP composite

of the inner layers, extending the surface observation at the MLC test. The decomposition curves of the composites aligned to the curve and temperature range of the PLA/APP reference sample, and similarly, all composites decomposed in one step. The clay-containing composites showed slightly lower thermal stability as their curves shifted to the left compared to the curve of the reference sample. Early thermal degradation of intumescent flame-retarded samples can promote the timely formation of the protective char layer delaying the ignition [5, 33]. The samples with 0.5 m/m% filler content noticeably show the greatest decomposition rate among the composites, and it is assumed that at such a low loading, the degrading effect of the metal ions in the clay minerals prevails (enhancing the degradation of the polymer), while at higher loading levels the clay particles are more ready to act together with the APP to form a flame-retardant system, overcoming their metal ions' unwanted degradation effect.

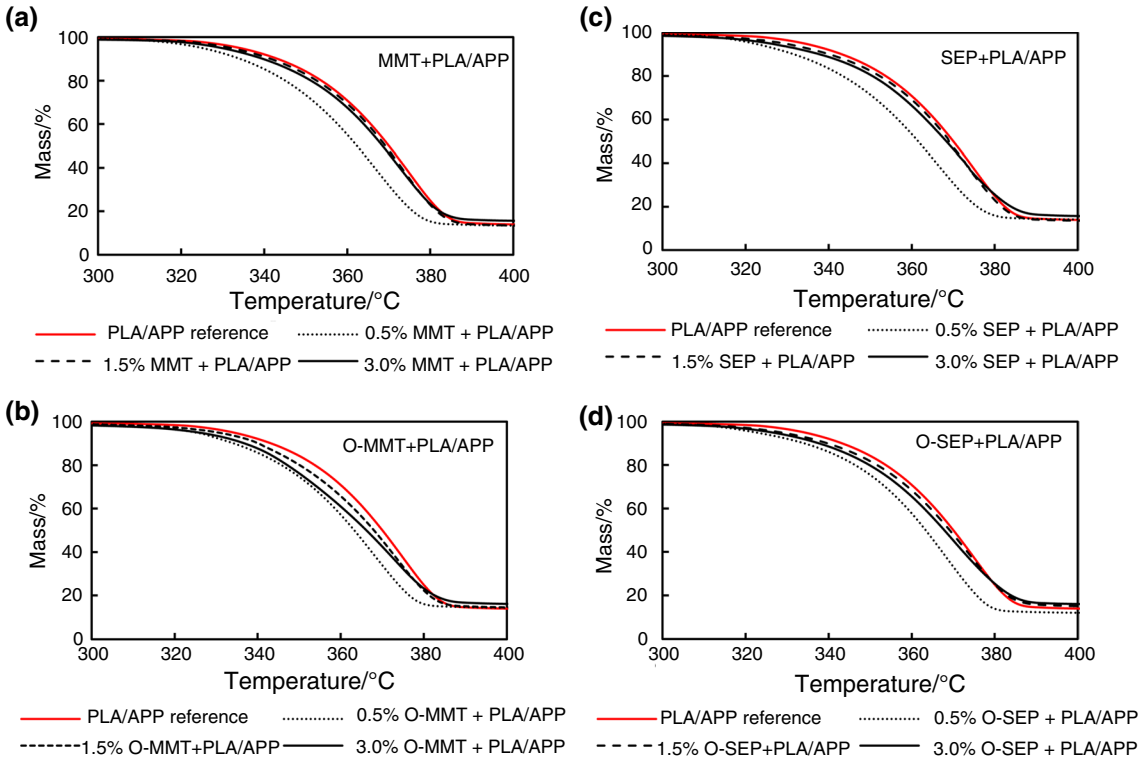

Fig. 4 The TGA curves of PLA/APP reference samples and the clay-incorporated composites; **a** MMT + PLA/APP, **b** O- MMT + PLA/APP; **c** SEP + PLA/APP; **d** O-SEP + PLA/APP

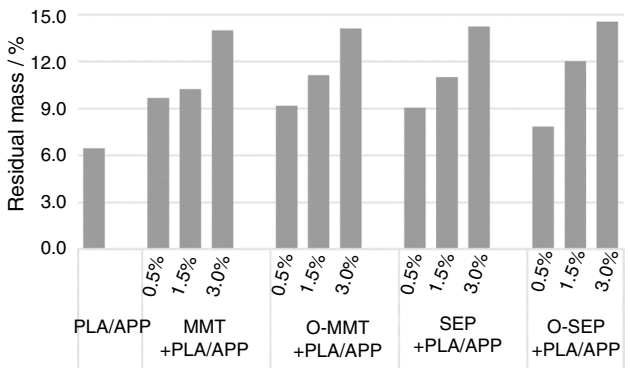

Fig. 5 Residual mass in TGA of the PLA/APP reference sample and the clay-containing composites

As seen in Fig. 5, with the increase of the clay content in the samples, the residual mass at 600 °C got greater, varying between 9 and 16% as opposed to the 6% residual mass of the reference sample. The presence of clay minerals is found to enhance the charring, and this is ascribed to the formation of the carbonaceous-silicate barrier layer by the clays in the composite, which can withhold the mass loss during the thermal degradation.

Table 3 The results of the LOI test for the PLA/APP reference sample and the clay-incorporated PLA/APP composites

PLA/APP reference	27		
Composite sample	LOI/v/v%		
	Clay loading level/m/m%		
	0.5	1.5	3.0
MMT + PLA/APP	35	35	34
O-MMT + PLA/APP	35	31	28
SEP + PLA/APP	34	32	27
O-SEP + PLA/APP	37	34	25

LOI test

The results of the LOI test for the PLA/APP reference sample and the clay-incorporated PLA/APP composites are shown in Table 3. The PLA/APP reference sample got an LOI value of 27 v/v%, while the highest LOI of 37 v/v% was reached by O-SEP + PLA/APP at 0.5 m/m% loading. Increasing the loading to 3 m/m% significantly reduced the ignition resistance of the composite. In regard to the loading level, this trend was observed for the other samples, too, and it was experienced in the literature as well [5, 32], except for the MMT clay-containing ones, where the LOI value

remained around 34–35 v/v%, showing steady performance for all loading levels. These results are consistent with the TTI results in the MLC test, where samples with the lowest loading level of 0.5 m/m% had the longest time to ignition (parallel with the highest LOI value), while composites with higher loading levels had shorted ignition time (and lower LOI values).

As witnessed in the TGA, the composites with the 0.5 m/m% loading had the highest mass loss as with the highest degradation. It is assumed that the bubbles formed as a result of the degradation rapidly transport the clay mineral particles to the surface, which then makes it difficult to ignite. However, the low clay content is not enough to form a durable protective layer under the long heat exposure in the MLC test, which resulted in higher pHRR and THR values. At the higher filler content, the increased heat conductivity due to the presence of the clays results in increased temperature and flammability; thus, lower LOI values and shorter ignition time were achieved. On the other hand, during the long heat exposure, the sufficient amount of clay fillers could form a durable barrier layer that could limit the propagation of fire. The exceptional LOI performance of MMT clays is presumed to its readiness for migration to the surface of the composite and effective charring ability there, which could overcome the flammability, while the O-MMT and the sepiolite clays, remaining in the matrix, could not limit the propagation of the fire on the top of samples.

Table 4 The results of the UL94 test for the PLA/APP reference sample and the clay-incorporated PLA/APP composites

PLA/APP reference	V-1		
Composite sample	UL94/-		
	Clay loading level/m/m%		
	0.5	1.5	3.0
MMT + PLA/APP	V-0	V-0	V-0
O-MMT + PLA/APP	V-2	V-1	HB
SEP + PLA/APP	V-2	V-0	HB
O-SEP + PLA/APP	V-2	V-0	HB

UL94

The results of the UL94 test for the PLA/APP reference sample and the clay-incorporated PLA/APP composites are shown in Table 4; the digital images of the observed samples in the UL94 test are shown in Fig. 6. When observing the effect of the loading level of clays, as an exceptional case, the MMT + PLA/APP composites showed steady performance at all loading levels as witnessed in the LOI test, achieving the required V-0 classification (Fig. 6). At 3.0 m/m%, the other composites achieved HB classification only as their burning period exceeded the burning time permitted for the vertical testing in the standard procedure (Fig. 6).

Both samples with SEP and O-SEP clays showed reduced dripping, while the O-MMT-containing one had burning drops that ignited the cotton underneath. The loading level of clays at 1.5 m/m% showed an optimal reduction of dripping and ignitability as the SEP + PLA/APP and the O-SEP + PLA/APP samples achieved V-0 classification, while O-MMT + PLA/APP got V-1. At 0.5 m/m% loading, these samples fell back to V-2 because at least one of the test specimens had flaming melt dripping (Fig. 6).

At 0.5 m/m% loading, the high mass loss rate (as seen from the TGA measurements) resulted in an increase in

Fig. 6 Digital images of the PLA/APP reference sample and the clay-incorporated PLA/APP composites in the UL94 test; IGN1: first ignition, IGN2: second ignition; image taken at the time passed after removing the flame source

dripping, as the degrading effect of the metal ions in the clay minerals prevails rather than their formation of flame-retardant system with APP at this loading level. Due to this, the drops were flaming and ignited the cotton pad, resulting in V-2 classification. At the 3.0 m/m% loading level, the increased flammability occurs because of the increased heat conductivity on the surface due to the higher content of the clay minerals. At 1.5 m/m% loading, the samples, due to their balanced behaviour, achieved V-0 and V-1 classifications. The MMT clay is presumed to have effective charring ability at the burning site on the surface of the sample, which can overcome the flammability, achieving the V-0 classification for all loading levels.

Conclusions

In order to enhance the efficiency of widely applied APP as an intumescent flame retardant in PLA, the synergic effect of clay minerals on the PLA/APP composite was examined. It was investigated whether the addition of the platelet-like structured montmorillonite or the sepiolite with microfibrous morphology had a better synergic impact, more so how the loading amount and the organomodification of these clays may affect the flame-retardant properties of PLA/APP composites.

When observing the morphology of clays, the sepiolites showed stronger interfacial interactions with the PLA matrix than the montmorillonites, and the organomodification improved the compatibility of the clay minerals according to the DMA results. In MLC, the best suppression of combustion was achieved by the composites with the 3 m/m% loading level of clay minerals, where the sepiolite-containing samples showed the most significant decrease in pHRR and THR values. Regarding organomodification, in the case of sepiolites, it proved beneficial as the O-SEP added composite achieved a 60% decrease in pHRR value and reduced the THR value to 60%. For montmorillonites, the improved compatibility by the organomodification with the PLA matrix seemed to hinder the rapid migration and accumulation of the clay minerals towards the surface of the polymer, reducing its effectiveness in the flame-retardant mechanism.

In the LOI and UL94 tests, reporting on the ignitability and dripping readiness of materials, only the less compatible nonmodified MMT could prevent the ignition at all the investigated concentrations. The increasing content for other clay additives resulted in decreased LOI values by 7–12 units and a fall back in the UL94 classification from V-0 to HB. It is concluded that ignition can be delayed with the low amount of clay that accumulates at the surface, while under sustained heat effect of combustion, the char reinforcing effect of organomodified fibrous clay is the most advantageous. Further studies are planned to confirm the structural reasons behind this behaviour.

Different conclusions can be drawn for each characterization method as the test methods inevitably examine different aspects of the samples — MLC for long excessive heat exposure, UL94 and LOI for flammability. In our conclusion, it is necessary to choose the appropriate method for characterizing the material in consideration of the criteria of the final applications and evaluate all of them to get a complex understanding. Overall, it was found that neat MMT clays can delay the ignition of the sample at a small loading. Meanwhile, incorporating O-SEP clay minerals at 3 m/m% loading results in great heat suppression, which is attributed to the significantly improved charring ability of the O-SEP + PLA/APP composites during the combustion.

Acknowledgements The project was funded by the National Research, Development and Innovation Fund of Hungary in the frame of the 2018-1.3.1-VKE-2018-00017, 2018-1.3.1-VKE-2018-00011, TKP2021-NVA-02, 2019–1.3.1-KK-2019–00004 and GINOP_PLUSZ-2.1.1-21-2022-00041 Projects. The research was funded by the Hungarian Scientific Research Fund, Grant Number FK128352.

Authors' contribution All authors contributed to the study conception and design. Material preparation, data collection and analysis were performed by Thuy Tien Nguyen Thanh, Beáta Szolnoki, Dániel Vadas, Milán Nacsa, György Marosi and Katalin Bocz. The first draft of the manuscript was written by Thuy Tien Nguyen Thanh, and all authors commented on previous versions of the manuscript. All authors read and approved the final manuscript.

Funding Open access funding provided by Budapest University of Technology and Economics.

Declarations

Conflict of interest The authors declare no conflict of interest.

References

1. Shumao L, Jie R, Hua Y, Tao Y, Weizhong Y. Influence of ammonium polyphosphate on the flame retardancy and mechanical properties of ramie fiber-reinforced poly(lactic acid) biocomposites. Polymer Int. 2010;59:242–8. https://doi.org/10.1002/pi.2715.
2. Yu T, Ren J, Li S, Yuan H, Li Y. Effect of fiber surface-treatments on the properties of poly(lactic acid)/ramie composites. Compos

A Appl Sci Manuf. 2010;41:499–505. https://doi.org/10.1016/j.compositesa.2009.12.006.
3. Rasal RM, Janorkar AV, Hirt DE. Poly(lactic acid) modifications. Progr Polymer Sci (Oxford). 2010. https://doi.org/10.1002/anie.201410770.
4. Iwata T. Biodegradable and bio-based polymers: Future prospects of eco-friendly plastics. Angewandte Chemie - Int Edition. 2015. https://doi.org/10.1002/anie.201410770.
5. Tang G, Deng D, Chen J, Zhou K, Zhang H, Huang X, et al. The influence of organo-modified sepiolite on the flame-retardant and thermal properties of intumescent flame-retardant polylactide composites. J Thermal Anal Calorim. 2017;130:763–72. https://doi.org/10.1007/s10973-017-6425-y.
6. Zhang J-F, Sun X. Mechanical properties of poly(lactic acid)/starch composites compatibilized by maleic anhydride. Biomacromol. 2004;5:1446–51. https://doi.org/10.1021/bm0400022.
7. Garlotta D. A literature review of poly(lactic acid). J Polym Environ. 2001;9:63–84. https://doi.org/10.1023/A:1020200822435.
8. Carrasco F, Pagès P, Gámez-Pérez J, Santana OO, Maspoch ML. Processing of poly(lactic acid): Characterization of chemical structure, thermal stability and mechanical properties. Polym Degrad Stab. 2010;95:116–25. https://doi.org/10.1016/j.polymdegradstab.2009.11.045.
9. Beheshti A, Heris SZ. Experimental investigation and characterization of an efficient nanopowder-based flame retardant coating for atmospheric-metallic substrates. Powder Technol. 2015;269:22–9. https://doi.org/10.1016/j.powtec.2014.08.048.
10. Södergård A, Stolt M. Properties of lactic acid based polymers and their correlation with composition. Progr Polymer Sci (Oxford). 2002. https://doi.org/10.1016/S0079-6700(02)00012-6.
11. Yu Y, Xi L, Yao M, Liu L, Zhang Y, Huo S, et al. Governing effects of melt viscosity on fire performances of polylactide and its fire-retardant systems. Science. 2022;25:103950. https://doi.org/10.1016/j.isci.2022.103950.
12. Bourbigot S, Fontaine G. Flame retardancy of polylactide: An overview. Polym Chem. 2010;1:1413–22. https://doi.org/10.1039/c0py00106f.
13. Tawiah B, Yu B, Fei B. Advances in flame retardant poly(lactic acid). Polymers. 2018. https://doi.org/10.3390/polym10080876.
14. Chow WS, Teoh EL, Karger-Kocsis J. Flame retarded poly(lactic acid): A review. Express Polymer Lett. 2018. https://doi.org/10.3144/expresspolymlett.2018.34.
15. John MJ. Flammability performance of biocomposites. Green Comp Autom Appl. 2018. https://doi.org/10.1016/B978-0-08-102177-4.00002-1.
16. Nazaré S, Kandola BK, Horrocks AR. Flame-retardant unsaturated polyester resin incorporating nanoclays. Polym Adv Technol. 2006;17:294–303. https://doi.org/10.1002/pat.687.
17. Morgan AB. Flame retarded polymer layered silicate nanocomposites: A review of commercial and open literature systems. Polym Adv Technol. 2006. https://doi.org/10.1002/pat.685.
18. Pluta M, Jeszka JK, Boiteux G. Polylactide/montmorillonite nanocomposites: Structure, dielectric, viscoelastic and thermal properties. Eur Polymer J. 2007;43:2819–35. https://doi.org/10.1016/j.eurpolymj.2007.04.009.
19. Jiang P, Zhang S, Bourbigot S, Chen Z, Duquesne S, Casetta M. Surface grafting of sepiolite with a phosphaphenanthrene derivative and its flame-retardant mechanism on PLA nanocomposites. Polymer Degrad Stab. 2019;165:68–79. https://doi.org/10.1016/j.polymdegradstab.2019.04.012.
20. Fukushima K, Fina A, Geobaldo F, Venturello A, Camino G. Properties of poly(lactic acid) nanocomposites based on montmorillonite, sepiolite and zirconium phosphonate. Express Polym Lett. 2012;6:914–26. https://doi.org/10.3144/expresspolymlett.2012.97.
21. Pluta M, Galeski A, Alexandre M, Paul MA, Dubois P. Polylactide/montmorillonite nanocomposites and microcomposites prepared by melt blending: Structure and some physical properties. J Appl Polym Sci. 2002;86:1497–506. https://doi.org/10.1002/app.11309.
22. Zhan J, Liu X, Yang T, Cao C. Flammability properties of intumescent flame retardant polylactic acid/layered silicate nanocomposites. IOP Conf Ser Earth Environ Sci. 2019. https://doi.org/10.1088/1755-1315/332/3/032046.
23. Li S, Yuan H, Yu T, Yuan W, Ren J. Flame-retardancy and anti-dripping effects of intumescent flame retardant incorporating montmorillonite on poly (lactic acid). Polym Adv Technol. 2009;20:1114–20. https://doi.org/10.1002/pat.1372.
24. Isitman NA, Kaynak C. Nanostructure of montmorillonite barrier layers: A new insight into the mechanism of flammability reduction in polymer nanocomposites. Polym Degrad Stab. 2011;96:2284–9. https://doi.org/10.1016/j.polymdegradstab.2011.09.021.
25. Fontaine G, Gallos A, Bourbigot S. Role of montmorillonite for enhancing fire retardancy of intumescent PLA. Fire Safety Sci. 2014;11:808–20. https://doi.org/10.3801/IAFSS.FSS.11-808.
26. He S. Organic modification of inorganic ions (Montmorillonite, Hydrotalcite) and its application in polylactic acid-based nanocomposites. IOP Conf Ser Earth Environ Sci. 2019. https://doi.org/10.1088/1755-1315/300/2/022109.
27. Ramesh P, Prasad BD, Narayana KL. Effect of MMT clay on mechanical, thermal and barrier properties of treated aloevera fiber/PLA-hybrid biocomposites. Silicon Silicon. 2020;12:1751–60. https://doi.org/10.1007/s12633-019-00275-6.
28. Hapuarachchi TD, Peijs T. Multiwalled carbon nanotubes and sepiolite nanoclays as flame retardants for polylactide and its natural fibre reinforced composites. Comp Part A Appl Sci Manuf. 2010;41:954–63. https://doi.org/10.1016/j.compositesa.2010.03.004.
29. Sinha Ray S, Okamoto M. Polymer/layered silicate nanocomposites: A review from preparation to processing. Prog Polym Sci (Oxford). 2003. https://doi.org/10.1016/j.progpolymsci.2003.08.002.
30. Liu M, Pu M, Ma H. Preparation, structure and thermal properties of polylactide/sepiolite nanocomposites with and without organic modifiers. Comp Sci Technol. 2012;72:1508–14. https://doi.org/10.1016/j.compscitech.2012.05.017.
31. Beheshti A, Heris SZ. Is MWCNT a good synergistic candidate in APP–PER–MEL intumescent coating for steel structure? Prog Organic Coatings. 2016;90:252–7. https://doi.org/10.1016/j.porgcoat.2015.10.023.
32. Guo Y, Chang CC, Cuiffo MA, Xue Y, Zuo X, Pack S, et al. Engineering flame retardant biodegradable polymer nanocomposites and their application in 3D printing. Polymer Degrad Stab. 2017;137:205–15. https://doi.org/10.1016/j.polymdegradstab.2017.01.019.
33. Hazer S, Coban M, Aytac A. Effects of the nanoclay and intumescent system on the properties of the plasticized polylactic acid. Acta Phys Pol, A. 2017;132:634–7. https://doi.org/10.12693/APhysPolA.132.634.
34. Norouzi M, Zare Y, Kiany P. Nanoparticles as effective flame retardants for natural and synthetic textile polymers: Application, mechanism, and optimization. Polym Rev. 2015;55:531–60. https://doi.org/10.1080/15583724.2014.980427.
35. González A, Dasari A, Herrero B, Plancher E, Santarén J, Esteban A, et al. Fire retardancy behavior of PLA based nanocomposites. Polym Degrad Stab. 2012;97:248–56. https://doi.org/10.1016/j.polymdegradstab.2011.12.021.

36. Isitman NA, Dogan M, Bayramli E, Kaynak C. The role of nanoparticle geometry in flame retardancy of polylactide nanocomposites containing aluminium phosphinate. Polym Degrad Stab. 2012;97:1285–96. https://doi.org/10.1016/j.polymdegradstab.2012.05.028.
37. Vadas D, Igricz T, Sarazin J, Bourbigot S, Marosi G, Bocz K. Flame retardancy of microcellular poly(lactic acid) foams prepared by supercritical CO2-assisted extrusion. Polym Degrad Stab. 2018;153:100–8. https://doi.org/10.1016/j.polymdegradstab.2018.04.021.
38. Patra S, Ajayan PM, Narayanan TN. Dynamic mechanical analysis in materials science: The Novice's Tale. Oxford Open Mater Sci. 2020. https://doi.org/10.1093/oxfmat/itaa001.
39. Bashir MA. Use of dynamic mechanical analysis (DMA) for characterizing interfacial interactions in filled polymers. Solids Multidiscip Digital Publ Inst. 2021;2:108–20. https://doi.org/10.3390/solids2010006.